Digestive Diseases and Sciences, Vol. 39, No. 5 (May 1994), pp. 1048–1054

Effects of Portacaval Anastomosis on Pancreatic Islets of the Rat

DANIELE BANI, MD, CAMILLO CORTESINI, MD, and TATIANA BANI SACCHI, DSc

The pancreatic islets of rats with surgically constructed end-to-side portacaval anastomosis were studied immunocytochemically, morphometrically, and ultrastructurally, and the plasma levels of glucose, insulin, and glucagon determined. The results of the current study show that, four weeks after surgery, hypoglycemia, normal insulinemia, and hyperglucagonemia occur and that these hematologic changes are associated with immunocytochemical and ultrastructural signs of impairment of the secretory activity of islet B cells and normal secretion pattern of the remaining islet cell types. The causes and the meaning of the hematologic and islet cell changes are discussed, and the hypothesis has been drawn that they are primarily related to the functional deterioration of the liver, which follows the diversion of the portal blood in the systemic circulation.

KEY WORDS: portacaval anastomosis; pancreatic islets.

End-to-side portacaval anastomosis (PCA) constructed surgically in the rat diverts hepatic blood supply from the portal vein to vena cava, thus creating a condition of atrophy and functional impairment of liver cells, which occurs within a few days from the intervention and persists for several months (1–11). Therefore, the rat with PCA can be regarded as an experimental model mimicking the conditions that occur in patients with liver failure, especially due to cirrhosis, and with portal–systemic shunt. The analogy between the experimental and the clinical condition is further strengthened by similar anatomical, behavioral, and biochemical changes in the central nervous system characteristic of hepatic encephalopathy (12).

Some endocrine consequences of PCA have been reported in the rat (10, 13), including abnormalities in glucose homeostasis and in plasma levels and secretion patterns of pancreatic hormones. In fact, it has been shown that basal plasma glucose is slightly reduced (14) and oral glucose administration results in an elevation of the maximal peak and a faster return to normal (3). Moreover, basal plasma insulin is normal, but oral glucose administration induces a greatly exaggerated insulin response (3). Finally, plasma glucagon is markedly elevated, and the insulin–glucagon ratio reduced (15). These alterations are accompanied by a dramatic reduction of hepatic glycogen stores (9, 14, 16–18), which, in turn, may also contribute to the abnormal carbohydrate metabolism found in PCA.

To what extent the above changes of glucose homeostasis and of plasma levels of pancreatic hormones are to be regarded as a consequence of the liver failure or of changes in the secretion pattern of the pancreatic islets, remains to be elucidated. The current research aims at investigating the possible role of the endocrine pancreas in determining the abnormalities of carbohydrate metabolism which take place upon PCA.

MATERIALS AND METHODS

Animals and Treatments. Ten adult male Wistar rats of the Nossan strain, weighing 200–250 g at the beginning of the experiment, were used. The experimental schedule was designed in compliance with the guidelines for animal

Manuscript received January 21, 1993; accepted April 26, 1993.

From the Department of Human Anatomy and Histology, Section of Histology, and 2nd Surgical Clinic, University of Florence, Florence, Italy.

Address for reprint requests: Prof. T. Bani Sacchi, Dipartimento di Anatomia Umana e Istologia, Sezione di Istologia "Enrico Allara," V. le G. Pieraccini, 6, I-50139 Firenze, Italy.

0163-2116/94/0500-1048$07.00/0

care and use of the University of Florence. The rats were purchased from a commercial dealer and acclimatized for seven days at 22–24° C on a 12-hr light–dark cycle. Standard laboratory chow and water were available *ad libitum*. The rats were divided in two groups of five animals each. At day 7 of harvesting (ie, day 1 of the experiment), the rats of the first group underwent end-to-side portacaval anastomosis (PCA) under diethyl ether anesthesia, according to Lee and Fisher (19). Interventions were performed between 4 and 6 PM. The unoperated rats of the other group were used as controls. All the animals were killed by cervical dislocation four weeks later. Access to food and water was interrupted 2 hr before killing. Upon sacrifice, the PCA rats were examined closely to confirm patency of the shunts.

Functional Analyses. Just prior to sacrifice, blood samples were collected from the tail vein in heparinized capillary tubes and immediately centrifuged to separate plasma. The basal plasma glucose levels were determined by the glucose oxidase method. The basal plasma levels of insulin and glucagon were determined by radioimmunoassay using kits supplied by Novo BioLabs (Bagsvaerd, Denmark).

Tissue Sampling. Upon sacrifice, fragments of pancreatic tissue coming from the juxtasplenic part of the pancreas were removed from each animal. Some of the specimens were fixed in Bouin's solution, dehydrated in graded ethanol, and embedded in paraffin. Other fragments were fixed in cold 4% glutaraldehyde in 0.1 M cacodylate buffer, pH 7.4, for 3 hr at room temperature and postfixed in cold 1% OsO_4 in 0.1 M sodium phosphate buffer, pH 7.4, at 4° C. The fragments were dehydrated in graded acetone, passed through propylene oxide, and embedded in Epon 812.

Immunocytochemistry. One Bouin's-fixed, paraffin-embedded tissue fragment (about 5 mm^3 in size) from each rat was used. Four serial sections 5 μm thick were placed on four separate slides. Similar series were prepared for the PCA rats and the controls. In each animal, the four slides were immunostained to reveal the four main islet hormones. The primary antisera used were as follows: anti-insulin (Novo; diluted 1:100), anti-pancreatic glucagon (Dako Patts, Santa Barbara, California; diluted 1:400), anti-somatostatin (Ortho, Raritan, New Jersey; diluted 1:1), and anti-pancreatic polypeptide (PP) (Dako Patts; diluted 1:1000). Anti-insulin was mouse monoclonal and immune reaction was revealed by the alkaline phosphatase–anti-alkaline phosphatase (APAAP) method (20). The remaining antisera were rabbit polyclonal and immune reaction was revealed by the avidin-biotin complex–alkaline phosphatase (ABC/AP) technique (21). New Fuchsin (Sigma, St. Louis, Missouri) was used to reveal AP activity. The immunostained sections were dehydrated in ethanol and mounted in Permount. The order for the immunostaining of the slides was insulin, glucagon, somatostatin, PP; thus, the sections stained with anti-PP serum were consecutive to those stained with anti-somatostatin serum, and so on. The specificity of the immunostaining was tested (1) by replacing the specific anti-hormone sera with nonimmune mouse/rabbit sera, and (2) by omitting the first layer.

Electron Microscopy. Ultrathin sections were cut from the Epon-embedded specimens and stained with uranyl-acetate and alkaline bismuth-subnitrate (22) and examined in a Siemens Elmiskop 102 electron microscope at 80 kV.

Morphometry. Computer-assisted morphometry was carried out on immunostained sections by a method employed previously by us for similar purposes (23). An Apple IIGS personal computer was used. It was interfaced with a Teleraster card (Pertel, Torino, Italy) to a CCTV television camera (Sony CCD) applied to a light microscope with a ×100 objective. The Teleraster card allows for the light transmitted across the immunostained histological section to be measured and a digitized image to be reproduced on the basis of the values estimated. In each rat, different, randomly chosen microscopic fields, each containing one islet or part of an islet, were recorded; five fields per hormone were considered in each of the PCA rats and the control rats. The software allows deletion from the digitized images of all parts corresponding to values of transmittance different from that of the immunostaining. In such a way, only the areas of the immunostained tissue components can be selected and then measured by determination of the number of pixels of the residual images. The program also allows the interactive tracing of the boundaries of the endocrine tissue on the digitized images and counting of the pixels of the encircled area. The values of the volume density of the immunostained areas, Vv (x/islet), were calculated as the ratio of x (number of pixels of the area immunostained for a given hormone) to islet (number of pixels of the area of islet tissue) in each image considered. For each hormone, the mean and SEM was computed for the PCA rats and for the control rats.

The values of the volume densities of ergastoplasm, Golgi apparatus, and secretory granules in B cells, Vv (x/cyto), were calculated as the ratio of x (number of points over the organelles considered) to cyto (number of points over the entire cytoplasm) by point counting on electron micrographs (24) at a ×10,000 final magnification. Five micrographs of B cells, coming from five different islets, were assayed in each PCA rat and control rat. An isotropic square lattice with distance between test points of 11.5 mm (equivalent to 1.5 μm on the section) was used. For each organelle, mean and SEM were calculated.

Statistical Analysis. Distribution of the morphometric values was normal when checked with the χ^2 test. Significance of differences between the PCA rats and the controls was evaluated by the Student's t test for unpaired values. $P < 0.05$ was considered significant.

RESULTS

Functional Assays. Compared with the controls, the rats with PCA reduced food consumption and, four weeks after surgery, had undergone a marked drop in body weight (265 ± 25 g vs 310 ± 15 g in the controls) and in liver mass, the latter accompanied by histologically detectable hepatocellular atrophy and depletion of glycogen stores (evaluated by PAS reaction). Moreover, biochemical alterations of the central nervous system, consisting with portosystemic encephalopathy, were also present in the same animals studied here (12).

Hematologic assays showed that in the rats with

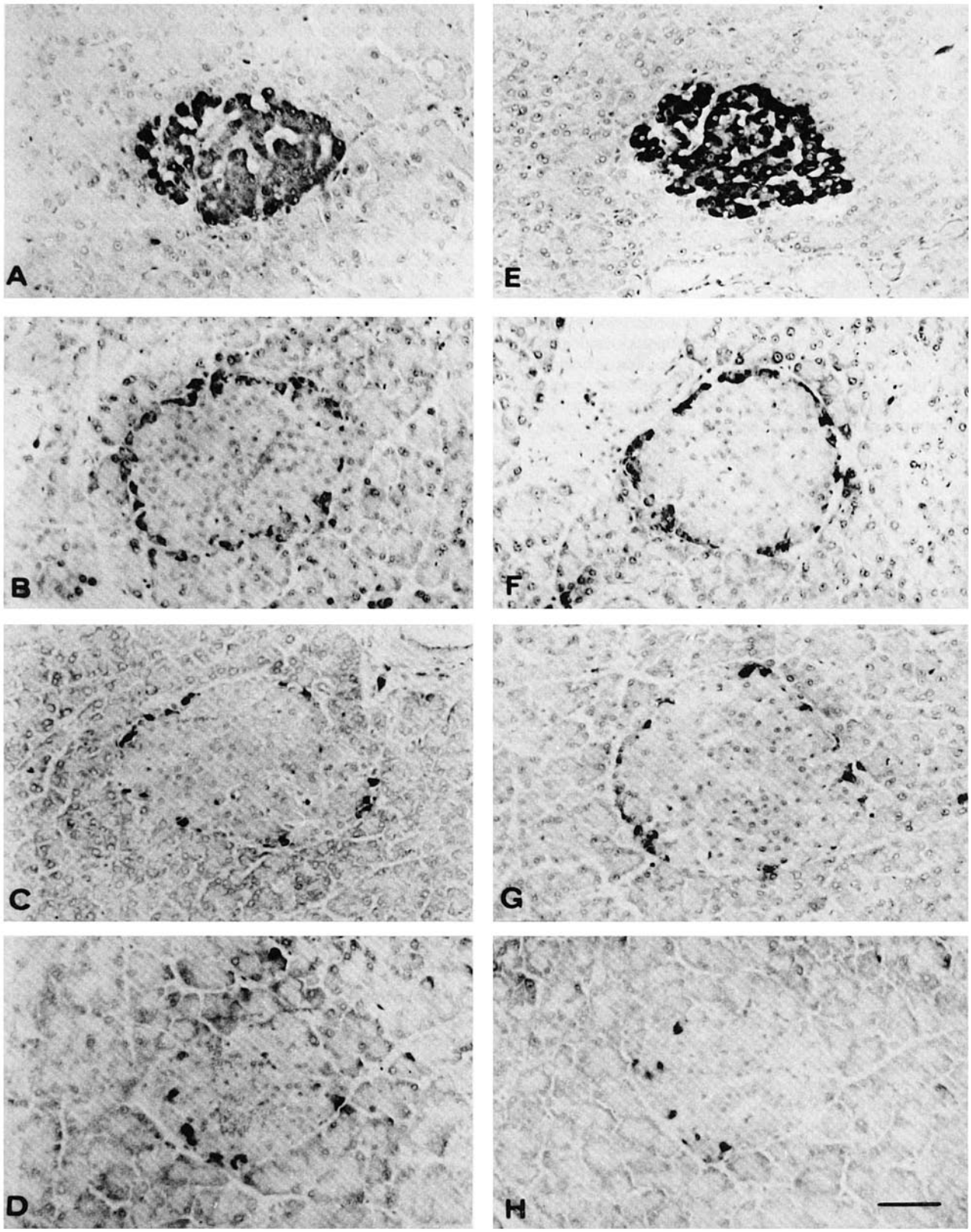

Fig 1. Islets from control (left) and PCA (right) rats. Immunostaining for insulin (A, E), glucagon (B, F), somatostatin (C, G), and PP (D, H). Immunoalkaline phosphatase method, counterstaining with Mayer's hemalum; ×240. Bar = 40 μm.

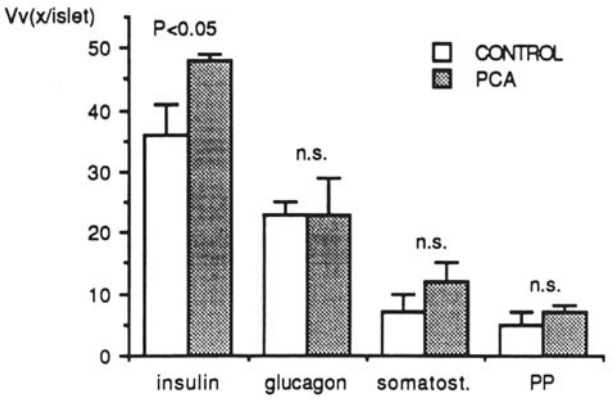

Fig 2. Histogram showing the volume densities of the immunoreactive islet hormones.

PCA, compared with the controls, plasma glucose was slightly but significantly reduced, plasma insulin was not significantly changed, and plasma glucagon was markedly and significantly increased (Table 1).

Morphology. By visual examination of the immunostained sections, the pancreatic islets from the control rats had all the well-known morphologic features of normal rat islets coming from the dorsal primordium. They showed a central core of B cells surrounded by a mantle formed by rather numerous A cells and minor amounts of D and PP cells (Figure 1 A–D). Most B cells were mildly immunostained. Conversely, the islets from the rats with PCA showed a majority of the B cells with very intense insulin immunoreactivity (Figure 1E). The other islet cell types did not appear to be substantially different from their control counterparts (Figure 1 F–H). The morphometric analysis carried out on the immunostained islets validated the above findings, showing a significant increase in the volume density of immunoreactive insulin, and no significant differences in the volume densities of immunoreactive glucagon, somatostatin, and PP (Figure 2). On electron microscopic examination, cytological changes of B cells were found in the islets of the rats with PCA compared with the con-

TABLE 1. HEMATOLOGIC PARAMETERS OF CONTROL AND PCA RATS

	Glucose (mg/dl)	*Insulin (μU/ml)*	*Glucagon (pg/ml)*
Controls	116 ± 3.8	9.9 ± 1.7	64.4 ± 8.9
PCA	95 ± 1.1	8.4 ± 1.4	295 ± 47
	$P < 0.001$	NS	$P < 0.001$

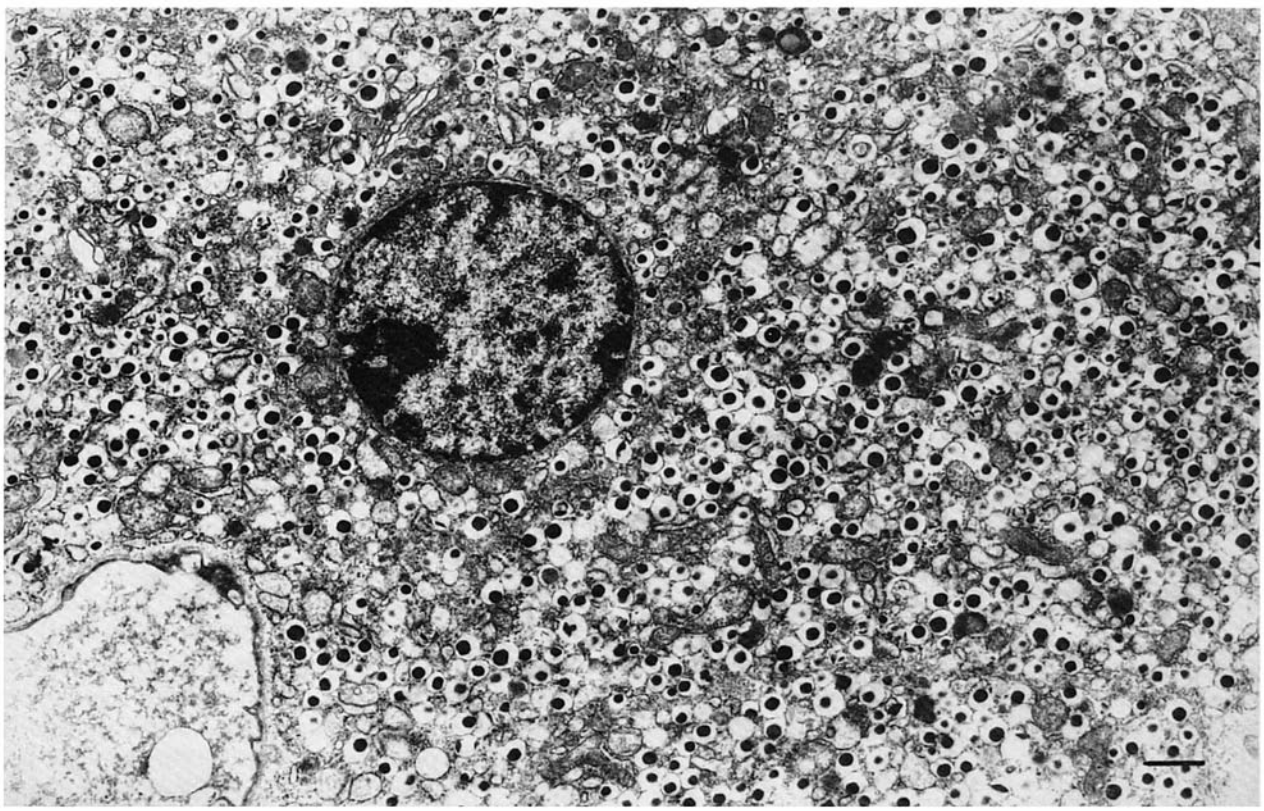

Fig 3. B cells from an islet of a PCA rat showing very numerous beta granules. Electron micrograph, ×7500. Bar = 1 μm.

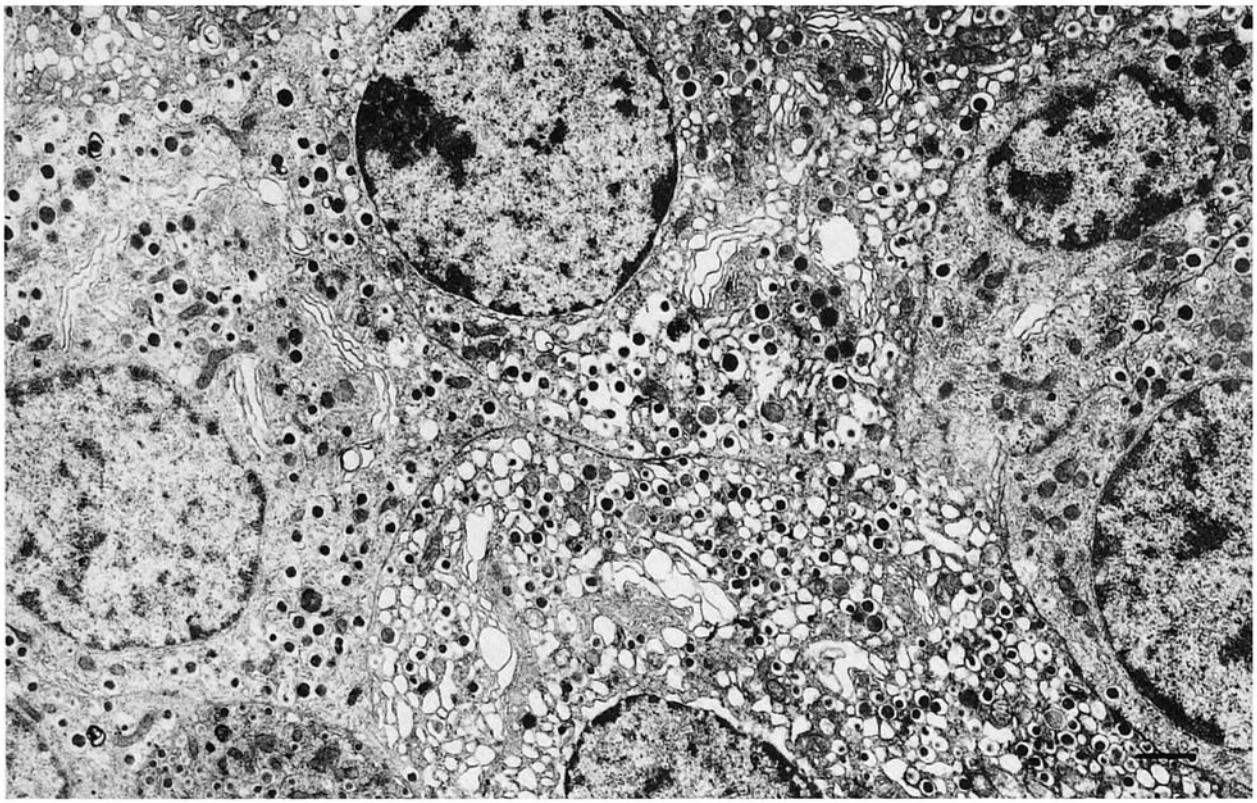

Fig 4. B cells from an islet of a control rat showing varying amounts of beta granules. Electron micrograph, ×7500. Bar = 1 μm.

trols. In fact, in the islets of the rats with PCA (Figure 3), most B cells contained very numerous beta granules, mainly of mature type with electron-dense cores, a moderately developed ergastoplasm, and a Golgi apparatus divided in small areas scattered throughout the cytoplasm. On the other hand, in the control islets (Figure 4), several B cells were rather poor in secretory granules, the ergastoplasm was usually well developed, and the Golgi apparatus occupied a single, large area near the nucleus. Ultrastructural morphometry revealed that, compared with the controls, the B cells of the rats with PCA showed a significant increase in the volume density of secretory granules and a significant decrease in the volume density of the ergastoplasm (Figure 5).

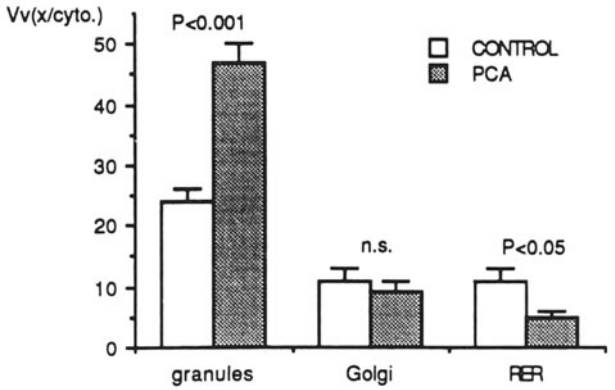

Fig 5. Histogram showing the volume densities of beta granules and organelles in B cells.

The non-B-cell types, including somatostatin-containing D cells and glucagon- and PP-containing non-B, non-D cells (25), had features quite similar in both control and PCA rats (Figure 6).

No signs of islet cell damage, inflammatory reaction, and *de novo* formation of endocrine cells outside the islets could ever be detected.

DISCUSSION

The current findings indicate that, following PCA, the pancreatic islets of the rat undergo changes consistent with increased storage of insulin in the B cells and depressed synthesis of secretory proteins. It is conceivable that this impairment in B-cell function is due to the persistent hypoglycemia. In spite of the apparent decrease of insulin secretion, the plasma levels of the hormone are not reduced. This is probably a consequence of diminished extraction of insulin by the atrophic liver cells

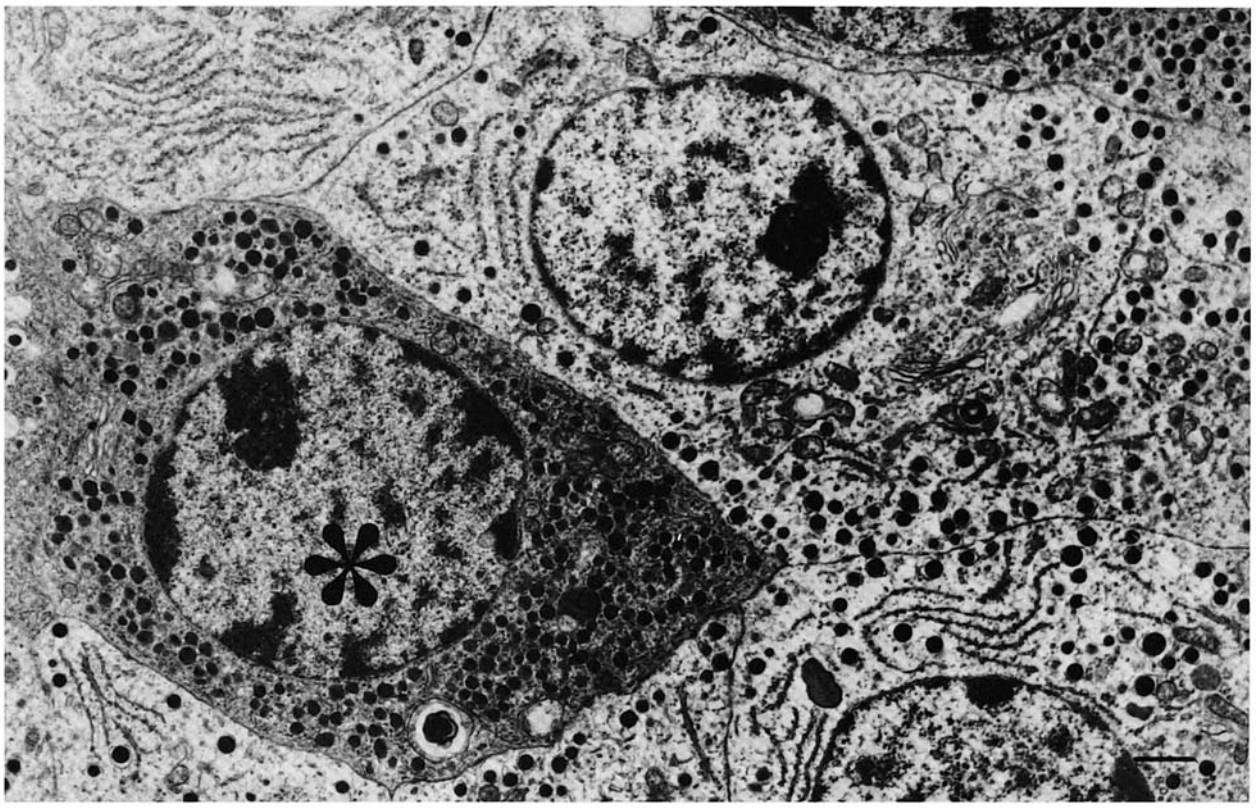

Fig 6. Some non-A, non-B cells (including glucagon- and PP-containing cells) and a D cell (asterisk) in the mantle of an islet from a PCA rat. Cytological features are quite similar to those of normal rats. ×7500. Bar = 1 μm.

and fits well with similar conclusions drawn by previous authors in studies on cirrhotic patients with PCA (26). The marked accumulation of insulin in B cells found by us in basal conditions may explain the exaggerated insulin response to oral glucose reported in previous studies (3).

The elevated plasma levels of glucagon in the PCA rats are associated with structural features of A cells indicating a normal secretion pattern. Hence, hyperglucagonemia does not seem to be caused by hypersecretion by islet A cells but, rather, by reduced catabolism of glucagon by the liver. The coexistence of hyperglucagonemia and hypoglycemia is probably related mainly to the functional impairment of the liver that, being almost completely devoid of glycogen, is no more able to adequately respond to glycogenolytic stimuli.

REFERENCES

1. Rubin E, Gervirtz NR, Cohan P, Tomita F, Jacobson JH: Liver cell damage produced by portacaval shunt. Proc Soc Exp Biol Med 118:235–237, 1965
2. Kyu MH, Cavanagh JB: Some effects of porto-caval anastomosis in the male rat. Br J Exp Pathol 51:217–227, 1970
3. Assal JP, Levrat R, Stauffacher W, Renold AE: Metabolic consequences of portacaval shunting in the rat: Effects on glucose tolerance and serum immunoreactive insulin response. Metabolism 20:850–858, 1971
4. Lauterburg BH, Sautter V, Preisig R, Bircher J: Hepatic functional deterioration after portacaval shunt in the rat. Gastroenterology 71:221–227, 1976
5. Mezzetti M, Contessini A, Avesani E, Santambrogio L, Mortara G, Agostini C: Studio del matabolismo proteico epatico in ratti portatori di derivazione porto-cavale termino-laterale. Policlinico Sez Chir 83:37–44, 1976
6. Dubuisson L, Saric J, Balabaud C, Bioulac P: Liver ultrastructure in the rat with portacaval shunt. A stereological study. Gastroenterology 79:1105, 1980
7. Pector JC, Winand J, DeHaye JP, Christophe J: Effects of portacaval shunt and transposition on fatty acids and cholesterol biosynthesis in rat liver. Am J Physiol 293:G83–G89, 1980
8. Dubuisson L, Bioulac P, Saric J, Balabaud C: Hepatocyte ultrastructure in rats with portacaval shunt. Dig Dis Sci 27:1003–1010, 1982
9. Pasquali Ronchetti I, Baccarani Contri M, Pittaluga S, Vassanelli P, Zannini P, Maruotti R: A morphometric and ultrastructrual study of the long term effect of portacaval anastomosis on the liver of normal male rats. J Submicrosc Cytol 15:731–749, 1983
10. Castaing D, Bismuth H: L'anastomose porto-cave chez le rat: 20 ans de modèle experimental. Gastroenterol Clin Biol 8:469–479, 1984

11. Dubuisson L, Bioulac-Sage P, Bedin C, Balabaud C: Hepatocyte ultrastructure in the rat after long term portacaval anastomosis: a morphometric study. J Submicrosc Cytol 16:283–287, 1984
12. Moroni F, Lombardi G, Carlà V, Pellegrini D, Carassale GL, Cortesini C: Content of quinolinic acid and of other tryptophan metabolites increases in brain regions of rats used as experimental models of hepatic encephalopathy. J Neurochem 46:869–874, 1986
13. Shih-Hoellwarth A, Lee C, Schwartz NB: Endocrine consequences of portacaval anastomosis in female rats. Am J Physiol 245:E288–E293, 1983
14. Rossouw JE, Labadarios D, Vinik A, De Villiers D: Liver glycogen after portacaval shunt in rats. Metabolism 27:1067–1073, 1978
15. Pector JC, Winand J, Verbeustel S, Hebbelinck M, Christophe J: Effects of portacaval diversion on lipid metabolism in rat adipose tissue. Am J Physiol 234:579–583, 1978
16. Starzl TE, Putnam CW, Porter KA, Halgrimson CG, Corman J, Brown BI, Gotlin RW, Rodgerson DO, Greene HL: Portal diversion for the treatment of glycogen storage disease in humans. Ann Surg 178:525–539, 1973
17. Marks C, Markey C, Dyer R, Vaupel MR: An electron microscopic study of the effects of portacaval shunts on the ultrastructure of the rat liver after partial hepatectomy. Am J Surg 129:156–162, 1975
18. Terlunen E, Altenahr E, Becker K, Ossenberg FW: Liver atrophy following portacaval shunt in normal rats. A morphometric study. Res Exp Med 170:133–142, 1977
19. Lee SH, Fisher B: Portocaval shunt in the rat. Surgery 50:668–672, 1961
20. Cordell JL, Falini B, Erber WN, Ghosh AK, Abdulaziz Z, Macdonald S, Pulford KAF, Stein H, Mason DY: Immunoenzymatic labeling of monoclonal antibodies using immune complexes of alkaline phosphatase and monoclonal anti-alkaline phosphatase (APAAP complexes). J Histochem Cytochem 32:219–229, 1984
21. Wood GS, Warnke R: Suppression of endogenous avidin-binding activity in tissues and its relevance to biotin-avidin detection systems. J Histochem Cytochem 29:1196–1204, 1981
22. Riva A: A simple and rapid staining method for enhancing the contrast of tissues previously treated with uranyl acetate. J Microsc 19:105–108, 1974
23. Bani D, Biliotti G, Bani Sacchi T: Morphological changes in the human endocrine pancreas induced by chronic excess of endogenous glucagon. Virchows Arch B Cell Pathol 60:199–206, 1991
24. Weibel ER: Stereological Methods, Vol. 1. London, Raven, 1979
25. Kaung HLC: Electron microscopic immunocytochemical localization of glucagon and pancreatic polypeptide in rat pancreas: Characterization of a population of islet cells containing both peptides. Anat Rec 212:292–300, 1985
26. Grilli F, Trevisani F, Bernardi M, De Palma R, Mazziotti A, Cavallari A, Patrono D, Gozzetti G, Gasbarrini G: Impairment of insulin secretion and metabolism after portal-systemic shunt (PSS) in cirrhotic patients. Gastroenterol Int 1(suppl 1):354, 1988 (abstract)